Mater. Res. Soc. Symp. Proc. Vol.1494 © 2013 Materials Research Society
DOI: 10.1557/opl.2013.236

Simulating Constant Current STM Images of the Rutile TiO_2 (110) Surface for Applications in Solar Water Splitting

F. F. Sanches[1], G. Mallia[1], and N. M. Harrison[1,2]
[1] *Thomas Young Centre, Department of Chemistry, Imperial College London, South Kensington London SW7 2AZ, UK*
[2] *STFC Daresbury Laboratory, Daresbury, Warrington, WA4 4AD, UK*

ABSTRACT

Solar water splitting has shown promise as a source of environmentally friendly hydrogen fuel. Understanding the interactions between semiconductor surfaces and water is essential to improve conversion efficiencies of water splitting systems. TiO_2 has been widely adopted as a reference material and rutile surfaces have been studied experimentally and theoretically. Scanning Tunneling Microscopy (STM) is commonly used to study surfaces, as it probes the atomic and electronic structure of the surface layer. A systematic and transferable method to simulate constant current STM images using local atomic basis set methods is reported. This consists of adding more diffuse p and d functions to the basis sets of surface O and Ti atoms, in order to describe the long range tails of the conduction and valence bands (and, thus, the vacuum above the surface). The rutile TiO_2 (110) surface is considered as a case study.

INTRODUCTION

Solar water splitting has shown a lot of promise as an environentally friendly source of hydrogen fuel. However, solar-to-fuel efficiencies have to be improved significantly for this to become a viable alternative to fossil fuels. A fundamental understanding of photoanode surface and water interaction could be essential in improving these efficiencies. TiO_2 is a commonly used semi-conductor for solar water splitting [1, 2]. Whilst the large bandgap of TiO_2 is somewhat prohibitive for widespread use, it has been widely adopted as a model material for experimental and theoretical study. In practice, nanostructured, predominantely anatase TiO_2 is most commonly used [3–5]. These systems are difficult to study at an atomic scale experimentally as well as computationally. However, pristeen clean surfaces of TiO_2 can be investigated with a number of experimental and theoretical techniques. These are useful as model systems, where the surface structure can be analysed, as well as the interaction of surfaces with adsorbates[6, 7]. Scanning Tunneling Microscopy (STM) is commonly used to study surfaces, as it probes the atomic and electronic structure of the surface layer.

The rutile (110) TiO_2 surface has been studied using STM previously [8, 9]. Experimentally, the observed bright spots are attributed to the surface undercoordinated Ti atoms. Theoretical studies played an important role in predicting/confirming this observation. The LDA approximation to DFT and the plane wave (pseudopotential) approach was used to reproduce these experimental results computationally by relaxing the surface structure and then simulating STM images [9].

It has been previously shown that the use of hybrid exchange functionals (where a proportion of Fock exchange is included in the exchange functional) gives an accurate description of the structural energetics and of the electronic structure (i.e. band gap and band offset) for periodic systems [10–21], particularly for transition metal oxides. The implementation of hybrid-exchange functionals using local atomic basis sets, as in the CRYSTAL code, is computationally efficient also for large periodic systems [22, 23]. Furthermore, local basis sets allow for a chemical description of molecular charge densities (eg. adsorbates on the surface). Di Valentin has demonstrated that using an atom-centered Gaussian basis set optimised for the ground state energy does not describe the long range tails of the valence and conduction bands in the vacuum above the surface sufficiently accurately [24]. In this study, the contrast in the STM image of the (110) surface is reversed with respect to previous calculations and experimental observations [9] (bright spots above the O atoms). In an attempt to remedy this and exploit the advantages of hybrid exchange functionals, additional s functions (called 'ghost functions') were added 2 Å above the x and y coordinates of the surface Ti and O (with the z axis perpendicular to the surface). The addition of these functions allows for more accurate description of the vacuum above the surface. This work has established the need to improve the description of the conduction band states for simulations of STM images. The approach of adding non-atom centred functions is unsatidfactory, however, as its application to complex surface geometries requires *ad hoc* decisions about positioning of the additional

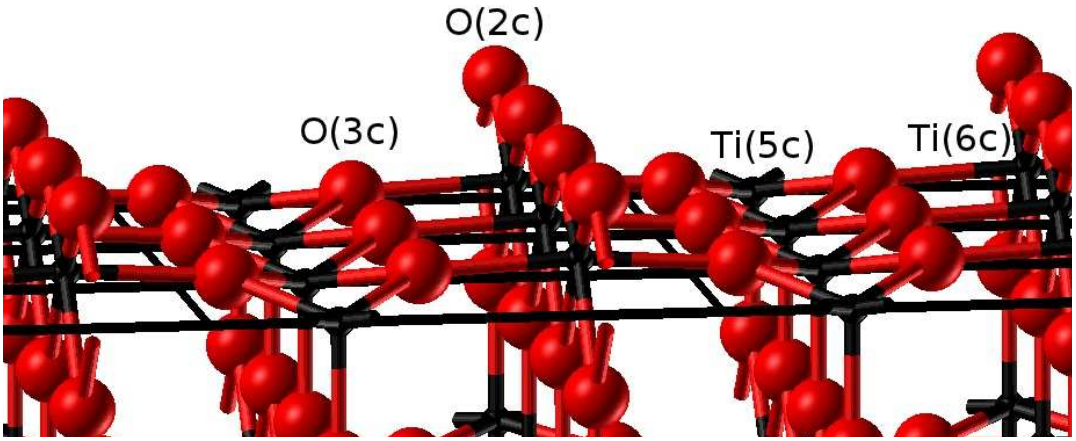

FIG. 1: 3D view of the rutile TiO_2 (110) surface. Small (large) spheres are titanium (oxygen) atoms. The surface cell lattice cell is also drawn. O(3*c*) and O(2*c*) are the three-fold (planar) and two-fold (bridging) coordinated oxygen ions. Ti(6*c*) and Ti(5*c*) are the six-fold and five-fold coordinated titanium ions.

basis functions.

Here, we propose an alternative method to improve the description of the long range tails of the valence and conduction bands and thus the description of the charge density in the vacuum. In principle, adding more diffuse functions to the atomic basis sets for the surface undercoordinated atoms should sufficiently improve the description of long range tails and achieve a similar effect described in Ref. [24]. This method could be more systematic and, perhaps, more transferrable to other surfaces/materials.

COMPUTATIONAL DETAILS

All calculations were performed using the CRYSTAL09 code[22], based on the periodic *ab initio* linear combination of atomic orbitals (LCAO). The hybrid exchange and correlation functional B3LYP [25] was adopted. A previous *ab initio* study of bulk rutile and anatase TiO_2 using various hybrid exchange correlation functionals showed that the B3LYP functional gave accurate descriptions of structural and electronic properties [26].

The atoms were described using local basis set (BS) consisting of atom centred Gaussian orbitals. Both the Ti and O atoms are described by a triple valence all-electron BS: an 86-411G** contraction (one *s*, four *sp*, and two *d* shells) and an 8-411G* contraction (one *s*, three *sp*, and one *d* shells), respectively; the most diffuse *sp*(*d*) exponents are α^{Ti}=0.3297(0.26) and α^{O}= 0.1843(0.6) Bohr^{-2}. Integration was carried out over reciprocal space using a shrinking factor of 8 to form a Pack-Mockhorst mesh of k points. This grid converges the integrated charge density to an accuracy of about 10^{-6} electrons per unit cell. The Coulomb and exchange series are summed directly and truncated using overlap criteria with thresholds of 10^{-7}, 10^{-7}, 10^{-7}, 10^{-7} and 10^{-14} as described previously [22, 27]. The self-consistent field (SCF) algorithm was set to converge at the point at which the change in energy, ΔE, was less then 10^{-7} Hartree.

DISCUSSION

Rutile (110) Surface

The rutile structure belongs to the $P4_2/mnm(D_{4h}^{14})$ tetragonal space group and the unit cell is defined by the lattice vectors $\mathbf{a_B}$ and $\mathbf{c_B}$ (the subscript B denoting the bulk phase) and contains two TiO_2 units with Ti ions at (0,0,0) and $(\frac{1}{2},\frac{1}{2},\frac{1}{2})$ and O ions at $\pm(u,u,0)$ and $\pm(u+\frac{1}{2},\frac{1}{2}-u,\frac{1}{2})$ [28, 29]. The predicted structural parameters, with the deviation from those observed [30] in parenthesis, are: $\mathbf{a_B}$ = 4.639Å(1.20%), $\mathbf{c_B}$ = 2.979Å(0.88%), u = 0.306(0.00%)

and $V_{\mathbf{B}} = 64.120\text{Å}^3(3.32\%)$. This structure is consistent with that predicted in previous calculations [28].
Each Ti is octahedrally coordinated to six O ions. The TiO_2 octahedron is distorted, with the length of the apical Ti-O_{ap} bonds slightly longer than equatorial, Ti-O_{eq}, bonds. The calculated (observed) lengths (in Å) being 2.009 (1.983) for Ti-O_{ap} and 1.959 (1.946) for Ti-O_{eq} [30].

The (110) surface displayed in Fig. 1 exposes three-fold (planar) and two-fold (bridging) coordinated oxygen ions, labelled as O($3c$) and O($2c$), and six-fold and five-fold coordinated titanium ions, labelled Ti($6c$) and Ti($5c$). A stoichiometric and non-polar termination is obtained by terminating such slabs on a bridging oxygen layer and only considering slabs consisting of multiples of 3 atomic layers according to the following sequence of planes: $O - Ti_2O_2 - O$. The effect of slab thickness on the surface structure and energy of formation has been carefully analysed and a full relaxation of slabs containing up to 36 atomic layers has been carried out.

Electronic Structure

The density of states (DOS) of the bulk rutile is displayed in Fig. 2(bottom), in which the contributions from two bands are evident: the top of the valence band and the conduction band. The valence band has predominantly O-$2p$ character but is hybridised with Ti-$3d$ orbitals. The conduction band is mainly derived from Ti-$3d$ atomic orbitals (with some hybridisation with O-$2p$ orbitals). Fig. 2(top) shows the DOS of the relaxed (110) surface. The calculated fundamental bandgap is very similar in both cases (3.41eV and 3.55eV for the bulk and surface, respectively). This is an indication that no surface states form in the band gap. The bulk band gap measured using optical techniqes is ∼3eV [31, 32]. The optical bandgap includes a contribution from excitonic binding which is not accounted for in the fundamental bandgap computed here. Therefore, the calculated values are in good agreement with this. The B3LYP functional gives a better estimate of fundamental band gaps in semi conductors than the commonly used LDA and GGA approaches [16, 33, 34].

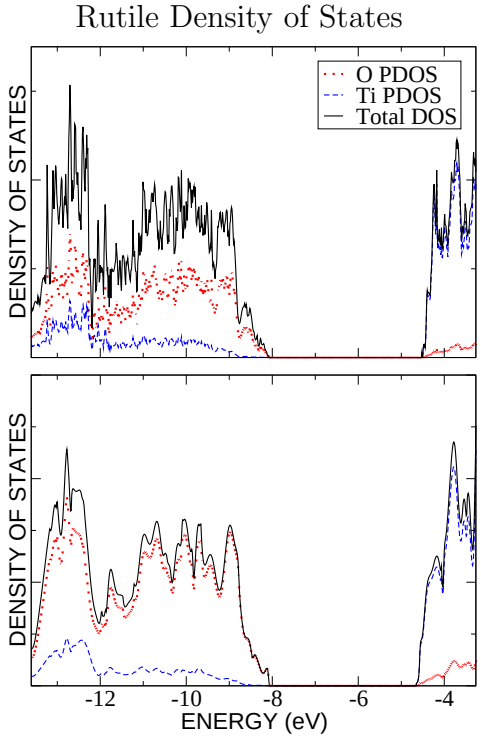

FIG. 2: (Colour on-line) Projected Density of States for bulk rutile (bottom) and the relaxed (110) surface (top). In both cases the continuous (black) line represents the total DOS, whilst the dotted (red) and dashed (blue) lines represent the DOS projected on all O and Ti atoms, respectively. The top of the VB of the bulk rutile was shifted to align with that of the (110) surface.

Simulated STM images

A systematic approach to optimising the basis sets for describing the long range tails of the conduction and valence bands (and, thus, the vacuum above the surface) has been adopted. This was achieved by adding more diffuse p and d functions to the basis sets of surface O and Ti atoms, respectively. Here we present a case study of the rutile TiO_2 (110) surface. We have also reproduced the calculations performed by Di Valentin for comparison [24].

The STM images were produced based on the Tersoff-Hamann approximation [35]. The interaction of tip and surface is ignored. The current is approximated as a charge density corresponding to the states in the lower part of the conduction band; an energy window, or bias potential, of 1V above the bottom of the conduction band is considered.

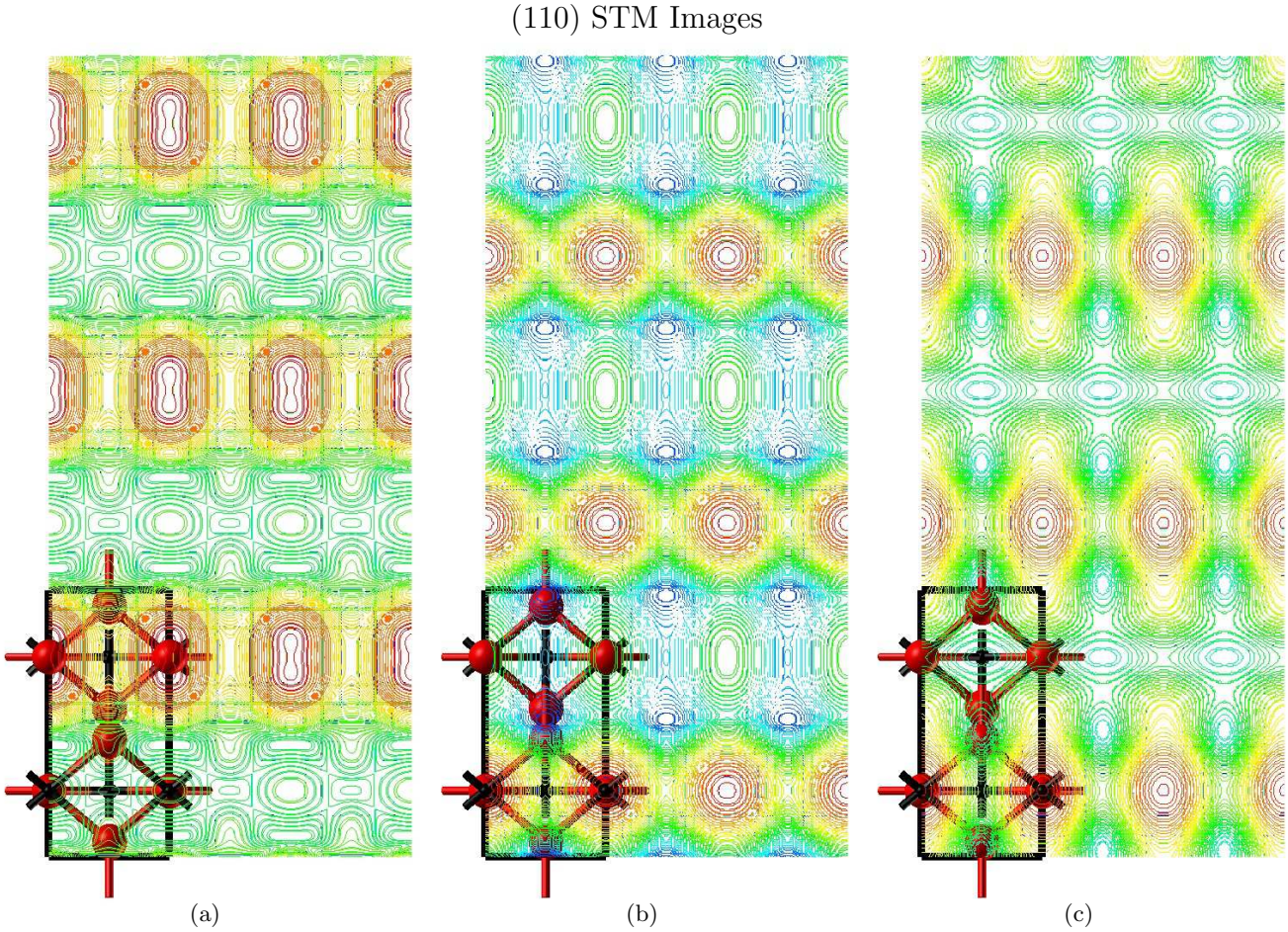

FIG. 3: (Colour on-line) Simulated constant current STM images for various basis set enhancements and the original BS. These are contour maps of the charge density isosurface at 5×10^{-6} electrons/bohr^3 and 1V sample bias. (a) Original Basis set (described in the computational details) (b) Original Basis set plus added s functions above the surface (c) Original Basis set with additional diffuse p and d functions in the surface O and Ti basis sets, respectively. In these images the largest values of height (red contours), comparable to bright spots on STM images, are located above the O atoms in (a) and in the region above the Ti atoms in (b) and (c).

In constant current STM images bright spots correspond to areas where surface topography and/or charge density has pushed the tip away from the sample (i.e. the height of the tip is increased). The contour plots shown in Fig. 3 are constant current contour plots. Red contours represent larger values of height (or bright spots on an STM image), whilst blue represents the lowest heights (dark areas). Examination of the position of the 'bright' areas on the three plots in Fig. 3 reveals that in a) the bright spots would be directly above the bridging oxygen atoms O(2c). This is in disagreement with the experimentally observed contrast, as well as previous (plane wave) calculations[8, 9]. This discrepancy is purely due to the inability of the basis set to describe long range conduction and valence band tails with sufficient accuracy. With the additional functions and enhanced atomic basis sets applied, (b) and (c) display

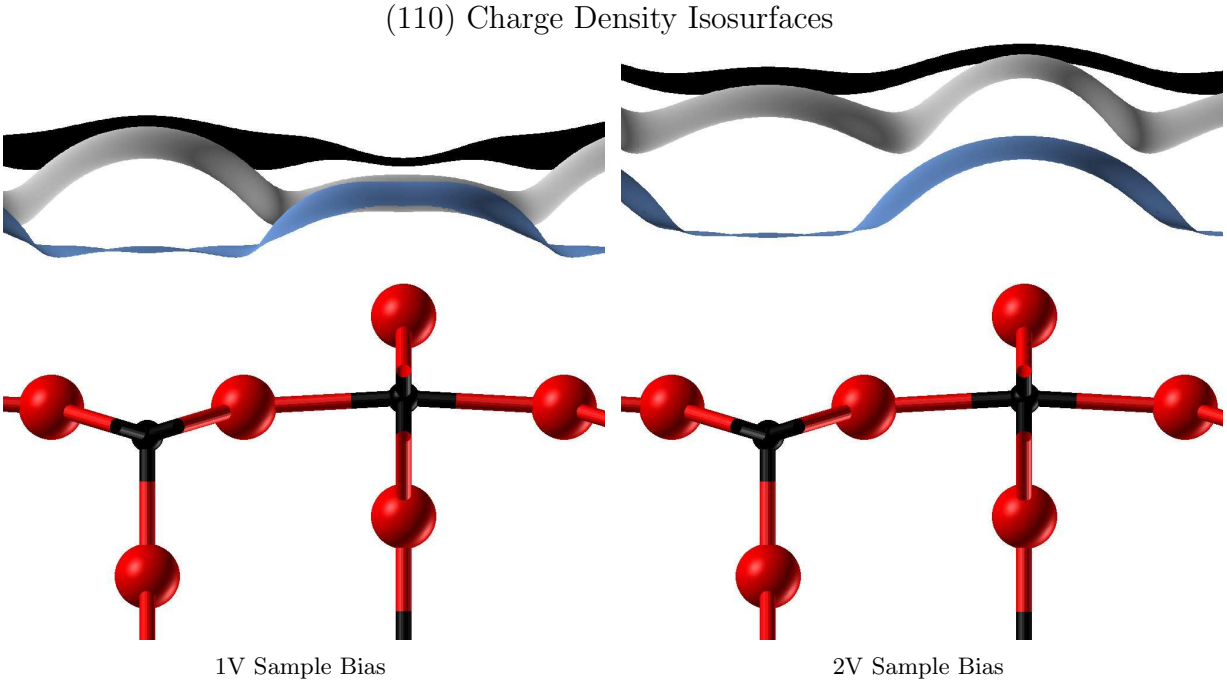

FIG. 4: (Colour on-line) Small (black) spheres represent Ti atoms and large (red) spheres represent O atoms. Traces above the atoms are charge density isosurfaces at 5×10^{-6} electrons/bohr^3. Above the titanium atom the traces represent from bottom to top: the isosurface obtained with the original BS (light blue); the isosurface obtained obtained after adding additional s functions above surface atoms (gray); the isosurface obtained after addition of diffuse p and d orbitals on the surface O and Ti BS respectively (black), respectively.

the expected contrast (bright spots above the Ti and dark(er) areas above the oxygen atoms.) Therefore, the method developed here produces results comparable to previous calculations [8, 24].

Analysis of the charge density isosurfaces at 2V applied bias in Fig. 4 reveals that in both the case of the enhanced atomic basis sets as well as the 'ghost atom' approach, the highest point remains above the O($2c$). We propose that sampling 2V above the bottom of the conduction band still includes regions where the description of the long range tails of the CB and VB are not described adequately. However, experimentally, a sample bias of 1V is commonly used to obtain high resolution STM images of TiO_2 surfaces [8, 9, 36]. Therefore, the use of 1V applied bias in the calculations is reasonable.

The isosurfaces at 1V applied bias reveal that using the basis set enhancements produces a broad peak centered around the Ti($5c$) and a trough directly above the O($2c$). In contrast, the 'ghost atom' approach produces two peaks above the Ti($5c$) and the O($2c$), where the latter peak is considerably smaller than the former. This would indicate bright spots above the titanium atoms in both cases. These observations are in line with the constant current contour plots in Fig. 3. Qualitative comparison of these isosurfaces with similar images in Ref. [8] appear to show better agreement between our method and the plane wave calculation than with the 'ghost atom' approach. The images produced by Diebold et. al. also show a peak above the titanium atom and a trough above the oxygen atom at comparable currents.

CONCLUSIONS

We have proposed an alternative approach to simulate constant current STM images using local atomic basis set methods. By enhancing the atom centred basis sets of the undercoordinated Ti and O atoms we avoid the need for additional functions above the surface. The approach was tested on the relaxed (110) surface and was found to produce similar contrast as in Ref [24]. The advantage of the approach we have presented here is that it provides a systematic and transferable method for the simulation of constant current STM images.

Acknowledgments

This work made use of the high performance computing facilities of Imperial College London and - via membership of the UK's HPC Materials Chemistry Consortium funded by EPSRC (EP/F067496) - of HECToR, the UK's national high-performance computing service, which is provided by UoE HPCx Ltd at the University of Edinburgh, Cray Inc and NAG Ltd, and funded by the Office of Science and Technology through EPSRC's High End Computing Programme.

---

[1] M. Gratzel, Nature **414**, 338 (2001).
[2] A. Fujishima and K. Honda, Nature **238**, 37 (1972).
[3] J. Tang, J. R. Durrant, and D. R. Klug, Journal of the American Chemical Society **130**, 13885 (2008).
[4] A. Cowan, J. Tang, W. Leng, J. Durrant, and D. Klug, The Journal of Physical Chemistry C **114**, 4208 (2010).
[5] A. M. Peir, C. Colombo, G. Doyle, J. Nelson, A. Mills, and J. R. Durrant, The Journal of Physical Chemistry B **110**, 23255 (2006).
[6] M. Patel, G. Mallia, and N. M. Harrison, in *NSTI NANOTECH 2011, TECHNICAL PROCEEDINGS - MICROSYSTEMS, PHOTONICS, SENSORS, FLUIDICS, MODELING, AND SIMULATION* , edited by Laudon, M and Romanowicz, B, (CRC PRESS-TAYLOR & FRANCIS GROUP, 6000 BROKEN SOUND PARKWAY NW, STE 300, BOCA RATON, FL 33487-2742 USA, 2011), ISBN , Nanotechnology Conference and Expo (Nanotech 2011), Boston, MA, JUN 13-16, 2011.
[7] M. Patel, G. Mallia, L. Liborio, and N. M. Harrison, Phys. Rev. B **86**, 045302 (2012).
[8] U. Diebold, J. Lehman, T. Mahmoud, M. Kuhn, G. Leonardelli, W. Hebenstreit, M. Schmid, and P. Varga, Surface science **411**, 137 (1998).
[9] U. Diebold, J. F. Anderson, K.-O. Ng, and D. Vanderbilt, Phys. Rev. Lett. **77**, 1322 (1996).
[10] D. Muñoz, N. M. Harrison, and F. Illas, Phys. Rev. B **69**, 085115 (2004).
[11] J. Muscat, A. Wander, and N. Harrison, Chemical Physics Letters **342**, 397 (2001).
[12] G. Mallia and N. M. Harrison, Phys. Rev. B **75**, 165201 (2007).
[13] N. C. Wilson, S. P. Russo, J. Muscat, and N. M. Harrison, Phys. Rev. B **72**, 024110 (2005).
[14] G. Mallia, R. Orlando, M. Llunell, and R. Dovesi, in *Computational Materials Science*, edited by C. Catlow and E. Kotomin (IOS Press, Amsterdam, 2003), vol. 187 of *NATO SCIENCE SERIES, III: Computer and Systems Sciences*, pp. 102–121.
[15] C. Di Valentin, G. Pacchioni, and A. Selloni, Phys. Rev. Lett. **97**, 166803 (2006).
[16] F. Corà, M. Alfredsson, G. Mallia, D. Middlemiss, W. Mackrodt, R. Dovesi, and R. Orlando, in *Principles and Applications of Density Functional Theory in Inorganic Chemistry II*, edited by N. Kaltsoyannis and J. McGrady (Springer Berlin / Heidelberg, 2004), vol. 113, pp. 171–232.
[17] G. C. De Fusco, L. Pisani, B. Montanari, and N. M. Harrison, Phys. Rev. B **79**, 085201 (2009).
[18] L. Liborio, G. Mallia, and N. Harrison, Phys. Rev. B **79**, 245133 (2009).
[19] C. L. Bailey, L. Liborio, G. Mallia, S. Tomić, and N. M. Harrison, Phys. Rev. B **81**, 205214 (2010).
[20] L. M. Liborio, C. L. Bailey, G. Mallia, S. Tomic, and N. M. Harrison, Journal of Applied Physics **109**, 023519 (pages 9) (2011).
[21] E. A. Ahmad, L. Liborio, D. Kramer, G. Mallia, A. R. Kucernak, and N. M. Harrison, Phys. Rev. B **84**, 085137 (2011).
[22] R. Dovesi, V. Saunders, C. Roetti, R. Orlando, C. Zicovich-Wilson, F. Pascale, B. Civalleri, K. Doll, N. Harrison, I. Bush, et al., Università di Torino (Torino, 2006).
[23] I. J. Bush, S. Tomi, B. G. Searle, G. Mallia, C. L. Bailey, B. Montanari, L. Bernasconi, J. M. Carr, and N. M. Harrison, Proceedings of the Royal Society A: Mathematical, Physical and Engineering Science **467**, 2112 (2011), http://rspa.royalsocietypublishing.org/content/early/2011/04/06/rspa.2010.0563.full.pdf+html.
[24] C. Di Valentin, The Journal of chemical physics **127**, 154705 (2007).
[25] A. Becke, Chem. Phys **98**, 5648 (1993).
[26] F. Labat, P. Baranek, C. Domain, C. Minot, and C. Adamo, The Journal of chemical physics **126**, 154703 (2007).
[27] C. Pisani, R. Dovesi, and C. Roetti, *Hartree-Fock ab initio Treatment of Crystalline Systems*, vol. 48 of *Lecture Notes in Chemistry* (Springer Verlag, Heidelberg, 1988).
[28] J. Muscat, V. Swamy, and N. Harrison, Physical Review B **65**, 224112 (2002).
[29] G. Cangiani, A. Baldereschi, M. Posternak, and H. Krakauer, Physical Review B **69**, 121101 (2004).
[30] U. Diebold, Applied Physics A: Materials Science & Processing **76**, 681 (2003).
[31] D. W. Fischer, Phys. Rev. B **5**, 4219 (1972).
[32] K. Hellwege and O. Madelung, Electron Paramagnetic Resonance, Springer-Verlag, Berlin (1984).
[33] R. Martin and F. Illas, Physical review letters **79**, 1539 (1997).
[34] I. de PR Moreira, F. Illas, and R. Martin, Physical Review B **65**, 155102 (2002).
[35] J. Tersoff and D. Hamann, Physical Review B **31**, 805 (1985).
[36] W. Hebenstreit, N. Ruzycki, G. Herman, Y. Gao, and U. Diebold, Physical Review B **62**, 16334 (2000).